# Reliable communication between rescuers during interventions using textile substrate-integrated-waveguide antenna systems

Thijs Castel[1], Sam Lemey[1], Sam Agneessens[1], Patrick Van Torre[1], Claude Oestges[2], Hendrik Rogier[1]
[1] Department of Information Technology, iMinds, Ghent University, Sint-Pietersnieuwstraat 41, B-9000 Ghent, Belgium
[2] Institute of Information and Communication Technologies, Electronics and Applied Mathematics, Université Catholique de Louvain, Place du Levant 3, B-1348, Louvain-la-Neuve, Belgium

***Abstract*—The safety of on-duty firefighters in indoor environments could be increased by ensuring reliable, high-data rate communication in potentially life-threatening situations. This increases their situational awareness, strengthens their decision making and decreases response time by ensuring efficient indoor communication of sensor data, biometrical data, pictures or videos. Therefore, a real-life rescue operation was replicated by means of two simultaneously moving firefighters in an office environment. These wideband channel sounder measurements were performed at 3.6 GHz with 80 MHz bandwidth. Four Ultra-Wideband Substrate Integrated Waveguide cavity-backed slot textile antennas were integrated in the front, back, left shoulder and right shoulder sections of the firefighters' jackets, providing up to $4 \times 4$ MIMO communication. For this indoor environment, we extract the pertinent OFDM parameters using the RMS delay spread and 50% correlation bandwidth of the sixteen individual SISO channels. Furthermore, we calculate the potential SISO-, $2\times2$ MIMO- and $4\times4$ MIMO-OFDM capacities and corresponding data rates. Finally, we show that the $4 \times 4$ MIMO setup is more energy efficient and increases both the link reliability and link quality.**

***Index Terms*—Body-to-body communication, MIMO-OFDM**

## I. Introduction

Recently, the National Protection Association has published their annual report, presenting firefighter fatalities in the United States for the year 2013 [1]. This report states, amongst others, that 27 firefighters were killed at 15 structure fires. This demonstrates the necessity to improve indoor wireless communication between firefighters in life-threatening situations. By ensuring highly reliable, efficient communication of sensor data, biometrical data, pictures or videos, rescue workers' safety is drastically increased.

This paper presents such a highly reliable broadband communication system between rescue workers, using textile Substrate Integrated Waveguide (SIW) antenna systems, which are unobtrusively and invisible integrated into the firefighter jackets. Therefore, broadband indoor body-to-body measurements, using the ULB-UCL elektrobit channel sounder, were performed between two simultaneously moving firefighters in an indoor office environment. From these measurements, which replicate real life rescue operations, the pertinent Orthogonal Frequency Division Multiplexing (OFDM) parameters are derived by means of the RMS delay spread and 50% correlation bandwidth. Moreover, the potential data rate for SISO, $2 \times 2$ MIMO up to $4\times4$ MIMO systems are calculated and compared. Additionally, the possible power reduction, when switching from $2 \times 2$ MIMO to a $4 \times 4$ MIMO setup, is analyzed. Measurements were performed at 3.6 GHz center frequency with 80 MHz OFDM bandwidth, which is the largest useful channel sounder bandwidth compatible with the IEEE 802.11 ac standard [2].

Some research on *narrowband* body-to-body channel characterization has been performed earlier. In [3], a comprehensive, statistical characterization for narrowband dynamic body-to-body communication channels at 2.45 GHz is described. Also in [4], indoor body-to-body channel gains, small-scale fading and large-scale fading are statistically described for narrowband measurements performed at 2.45 GHz. When focusing on *wideband* channels, [5] describes the channel characterization of wideband body-to-body channels by means of static and dynamic measurements. More wideband channel simulations are presented in [6], studying the performance gain when going from SISO Multiband (MB)-OFDM to MIMO MB-OFDM for a body-surface node to an external node, defined as *off-body* communication. In [7], the optimum *on-body* locations for static and pseudo dynamic measurements scenarios are determined for an MB-OFDM UWB body-centric wireless network.

To our knowledge, this is the first analysis of indoor broadband body-to-body communication channels between two simultaneously moving firefighters in an office environment, calculating the pertinent OFDM parameters and the $2 \times 2$ and $4 \times 4$ MIMO-OFDM capacities. Section II presents the Ultra Wideband SIW antenna, the measurement scenario and channel sounder settings. Section III describes the calculation of the RMS delay spread and 50% correlation bandwidth further used in Section IV to derive the pertinent OFDM parameters. Section V presents the calculated MIMO-OFDM capacities. Finally, the conclusions are drawn in Section VI.

## II. Measurement setup

To perform reliable broadband body-to-body measurements, an Ultra Wideband cavity backed-slot antenna in Substrate Integrated Waveguide (SIW) technology was designed in [8]. This antenna design provides stable radiation characteristics when the firefighter is performing a real life rescue operation. Since the antenna is fabricated using low-profile, light-weight

and flexible antenna materials, the textile antenna is easily and unobtrusively imtegrated inside the firefighter jackets. Moreover, while the antenna design ensures high isolation from the human body, the SIW textile antenna also yields excellent performance when placed at the four on-body locations used for the measurements. The designed UWB cavity backed-slot antenna in SIW technology is matched for the frequency band ranging from 3.33 GHz to 4.66 GHz, with a -10 dB bandwidth of 1.33 GHz and a fractional bandwidth of 33%. More antenna characteristics and dimensions are described in [8]. Both the TX and RX firefighters are equipped with four SIW UWB textile antennas, integrated in the front, the back, the left shoulder and the right shoulder sections of the firefighter jackets, as shown in Fig. 1, providing up to $4 \times 4$ MIMO. Note that the on-body antenna locations guarantee minimal influence on antenna performance caused by firefighter movement or by the oxygen bottle and buckles worn by the firefighters.

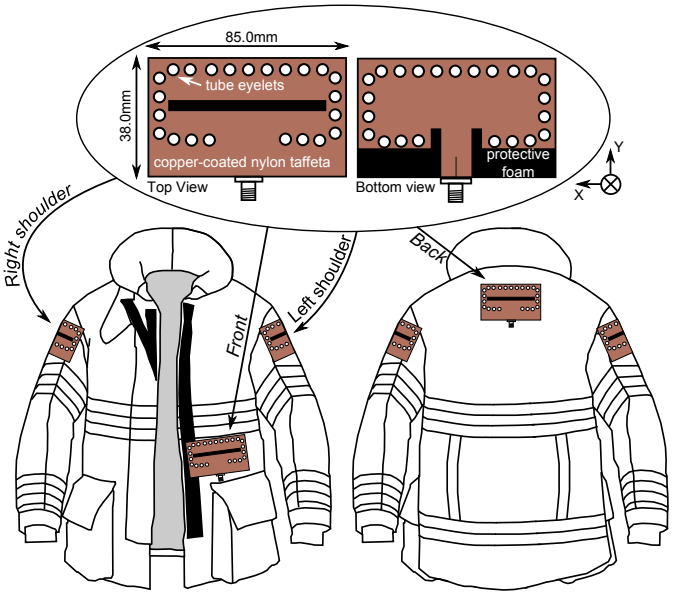


Fig. 1. On-body locations of the four integrated UWB SIW textile antennas, for both the TX and RX firefighter.

Mobile measurements were performed with both firefighters simultaneously moving in an indoor office environment. Special care was taken that the measurement scenario replicates real life rescue operations by simulating the scenario where the TX firefighter, whose trajectory is marked by the long dashed line on Fig. 2, is scanning the hallway while the RX firefighter, whose trajectory is marked by the short dashed line, is simultaneously scanning the offices. The markers A, B and C, placed along the TX and RX firefighter trajectories, indicate where both firefighters are located at the same time instance. Moreover, the subintervals ① to ④ are used to indicate different propagation phenomena depending on the mutual position and orientation of both firefighters.

Measurements were performed at 3.6 GHz center frequency with 80 MHz OFDM bandwidth. The TX power of the ULB-UCL channel sounder was chosen 1mW to ensure good timing synchronization and frequency offset estimation, as explained in Section V.

## III. Channel Characterization

Indoor body-to-body communication experiences a large influence of multiple delayed paths arriving at the RX firefighter, caused by several reflectors and scatterers. The power delay profile $P_h(\tau)$ shows the power and the corresponding delays of these delayed paths, defined as multipath components, together with the power and the delay of the dominant, strongest path. Both the power and delays of the dominant and the multipath components dramatically depend on the mutual orientation and the relative position of both firefighters, as shown in Fig. 3, which presents the time-varying behaviour of $P_h(\tau)$ for the back to back (B2B) SISO link.

At the beginning of subinterval 1, the received signal power on the RX back antenna is maximal since the back antennas of the TX and RX firefighter are approximately side by side, yielding a strong Line of Sight link. When both firefighters start walking, the power level slowly decreases because of the extra path loss and because the Line of Sight link is changing in a Non Line of Sight link. At the beginning of subinterval 2, the received signal power drastically drops because the RX firefighter has rotated, introducing body shadowing effects. Moreover, the RX back antenna is now pointing away from the TX back antenna. In interval BC, both firefighters are walking in the corridor along the same positive X direction. Now, strong multipath components arise, as indicated by the red circles on Section C-60 in the inset of Fig. 3. Moreover, as an example, one dominant multipath component, denoted by the dashed line on Fig. 3, clearly increases in delay and path length, indicating that it is caused by a strong reflection at the beginning of the corridor.

Based on the power delays presented in Fig. 3, the Root Mean Square (RMS) delay spread and the 50% correlation bandwidth of this B2B SISO channel are calculated, further used to determine the cyclic prefix length and subcarrier bandwidth when applying OFDM. Furthermore, since we focus on $2 \times 2$ and $4 \times 4$ MIMO, the channel parameters of all sixteen SISO links should be determined separately.

*1) **RMS delay spread**:* The RMS delay spread $\tau_{RMS}$ indicates the time domain spread of multiple delayed copies of the transmitted pulse and is calculated for every measurement cycle, for all sixteen SISO links separately, with respect to the mean delay $\bar{\tau}$ [9]:

$$\bar{\tau} = \frac{\sum_{l=1}^{L} P_l.\tau_l}{\sum_{l=1}^{L} P_l} \tag{1}$$

$$\tau_{RMS} = \sqrt{\frac{\sum_{l=1}^{L} P_l.(\tau_l - \bar{\tau})^2}{\sum_{l=1}^{L} P_l}} \tag{2}$$

With *L* the number of distinct multipath components, $P_l$ the power of a multipath component and $\tau_l$ the corresponding delay of that multipath component. Table I shows the 10% outage probability of the calculated RMS delay spreads, denoted as

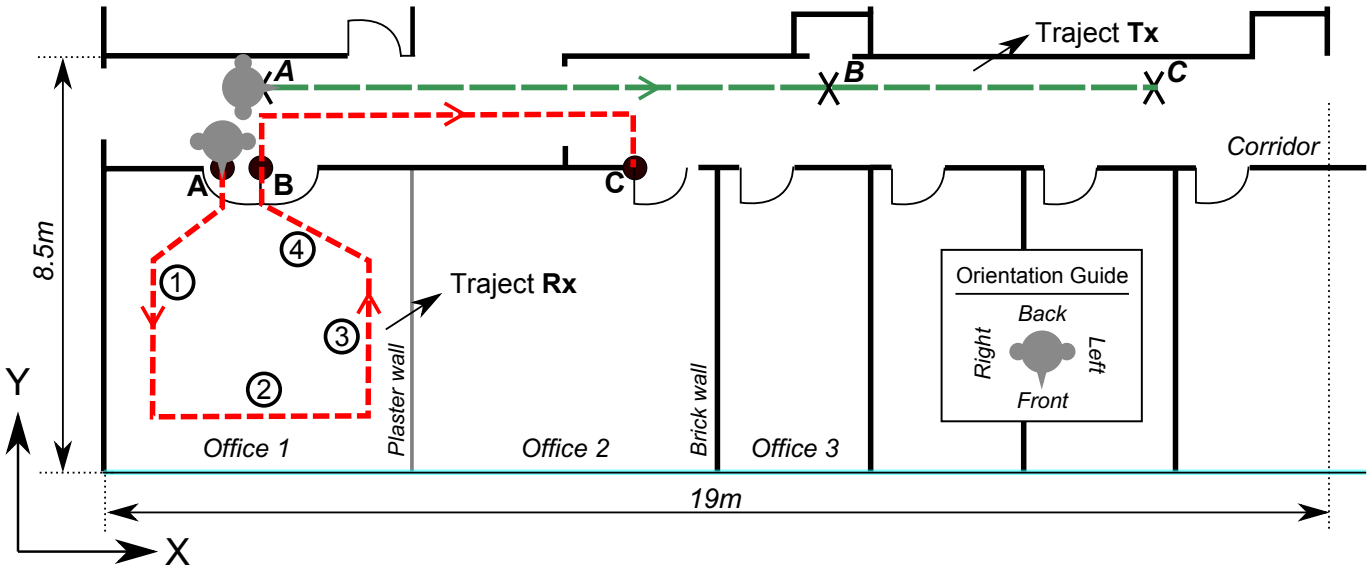


Fig. 2. Simplified floor plan with the wideband body-to-body measurement scenario

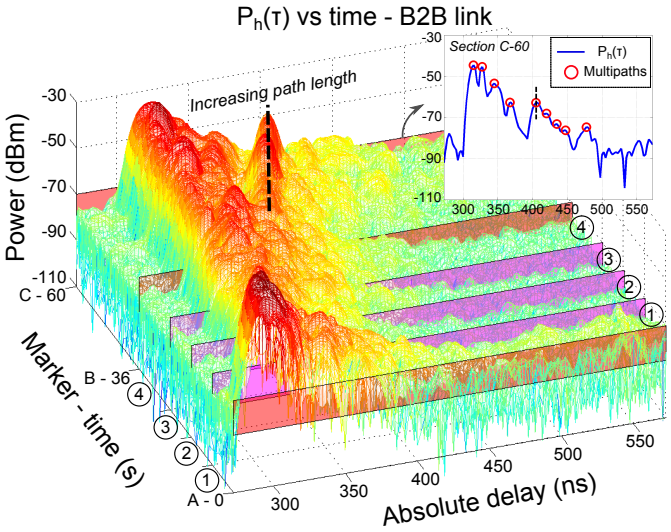


Fig. 3. Time varying power delay profile $P_h(\tau)$ for the back to back link together with $P_h(\tau)$ of the last measurement cycle, corresponding to time instance C-60.

$\tau_{RMS,10}$, for every SISO link separately. This 10% outage probability level is defined as the maximal $\tau_{RMS}$ during 90% of the time and is further used to determine the cyclic prefix length when applying OFDM. For example, the RMS delay spread of the front to back link is below 45.80 ns during 90% of the time. Previous extensive wideband indoor channel measurements, described in [10], show that $\tau_{RMS}$ is environment and frequency dependent, with values generally below 30 ns, except for very large rooms with large distances between possible reflectors, as is the case in this indoor environment. A more general rule of thumb indicates that $\tau_{RMS}$ is above 10 ns and under 50 ns [9] for indoor environments, which is confirmed by our calculations.

*2) **50% correlation bandwidth**:* If $\tau_{RMS}$ is not significantly smaller than the symbol duration $T_S$, consecutive symbols influence each other. This leads to Inter Symbol Interference (ISI) and frequency selective fading, described by observing the frequency correlation function $R_T(\Delta f)$ calculated as the the Fourier Transform of $P_h(\tau)$ [9]:

$$R_T(\Delta f) = \int_0^{\tau_{max}} P_h(\tau).e^{-j2\pi\Delta f\tau}.d\tau \qquad (3)$$

In this paper, the 50% correlation bandwidth $B_{C,0.5}$ is defined as the minimal bandwidth separation $\Delta f$, resulting in 50% correlation (or -3dB). Table I shows the 10% outage probability of the calculated 50% correlation bandwidths, for every SISO link separately. This 10% outage probability level is defined as the minimal $B_{C,0.5}$ during 90% of the time and is further used to determine the subcarrier spacing when applying OFDM. For example, $B_{C,0.5}$ of the left shoulder to back link is larger then 3.53 MHz during 90% of the time.

## IV. OFDM PARAMETERS

To avoid Inter Symbol Interference (ISI), the symbol duration $T_S$ is chosen sufficiently larger than the RMS delay spread $\tau_{RMS}$. However, increasing $T_S$ results in a lower data rate, which limits the possibility to transmit live sensor and biometrical data, pictures or video between two firefighters. Therefore, the frequency selective wideband channel is subdivided into $N$ frequency-flat subcarriers, ensuring large data rates without introducing ISI. The bandwidth $\Delta$f of these frequency-flat subcarriers is typically chosen smaller than one tenth of the coherence bandwidth $B_{C,0.5}$ [9] whereas the cyclic prefix CP is chosen larger than three times $\tau_{RMS}$ [11] to ensure that consecutive symbols on the same subcarrier do not interfere.

Using $\tau_{RMS,10}$ and $B_{C,0.5,10}$, presented in Table I, the pertinent OFDM parameters for the wideband body-to-body channel are determined. For a practical implementation, only one set of values for $\Delta$f and CP is chosen, guaranteeing frequency-flat fading and preventing ISI, during 90% of the

TABLE I
10% OUTAGE PROBABILITY OF $\tau_{RMS}$, IN NS, AND 10% OUTAGE PROBABILITY OF $B_{C,0.5}$, IN MHZ

| | $\tau_{RMS,10}$ $P(\tau_{RMS} < \tau_{RMS,10}) = 0.9$ | | | | $B_{C,0.5,10}$ $P(B_{C,0.5} > B_{C,0.5,10}) = 0.9$ | | | |
|---|---|---|---|---|---|---|---|---|
| RX → | F | B | L | R | F | B | L | R |
| TX Front | 33.10 | **45.80** | 34.03 | 17.59 | 8.63 | 3.92 | 8.63 | 11.76 |
| TX Back | 19.68 | 17.62 | 18.63 | 25.66 | 8.63 | 11.76 | 12.16 | 8.63 |
| TX Left | 25.47 | 36.29 | 28.54 | 19.67 | 5.10 | **3.53** | 9.41 | 9.80 |
| TX Right | 18.99 | 29.83 | 20.05 | 31.60 | 11.37 | 5.49 | 10.59 | 3.92 |

time, in all sixteen SISO links. Therefore, the stringent limit, being the smallest $B_{C,0.5}$, which determines $\Delta f_{max}$, and the largest $\tau_{RMS}$, which determines $CP_{min}$, are chosen. This results in next OFDM parameters:

$$CP_{min} = 3.\tau_{RMS,max} = 137.4ns \tag{4}$$

$$\Delta f_{max} = \frac{1}{10}.B_{C,0.5,min} = 353kHz \tag{5}$$

These calculated OFDM parameters are compatible with the 802.11 ac standard [2], which defines the minimal cyclic prefix length equal to 400 ns, being larger than the $CP_{min}$, and the subcarrier bandwidth equal to 312.5 kHz, being smaller than $\Delta f_{max}$.

## V. MIMO-OFDM CAPACITY

For the MIMO-OFDM capacity calculations, the 80 MHz indoor body-to-body channel is subdivided into 256 frequency-flat subcarriers, with their subcarrier bandwidth equal to 312.5 kHz, corresponding the the 802.11 ac standard. The capacity for subcarrier *k*, when assuming constant TX power with constant power spectral density and employing uniform power allocation, is then calculated as:

$$C_k = \log_2\left(\det\left[\mathbf{I}_{N_{RX}} + \frac{P_k}{N_{TX}.\sigma^2}.\mathbf{H_k}.\mathbf{H_k}^H\right]\right). \tag{6}$$

With $P_k$ the transmit power allocated to the *k*-th subcarrier, $\sigma^2$ the noise power, $\mathbf{H_k}$ the channel matrix of the *k*-th subcarrier, $N_{TX}$ the number of transmit antennas and $N_{RX}$ the number of receive antennas. Using these subcarrier capacities $C_k$, the OFDM capacity $\bar{C}_{\text{OFDM}}$ [bps/Hz] is calculated as the average over all *N* subcarrier capacities [12]–[14]:

$$\bar{C}_{\text{OFDM}} = \frac{1}{N}\sum_{k=1}^{N} C_k. \tag{7}$$

Since all sixteen SISO links vary independently owing to the constantly varying mutual orientation and relative position of each firefighter as well as people moving in the environment, we first look at the 10% outage SNR of each SISO link, being the SNR guaranteed 90% of the time. According to [15], the SNR of such a SISO link should be larger than, or equal to, 5 dB to guarantee reliable timing synchronisation and frequency offset estimation for all SISO links in MIMO-OFDM systems. Therefore, we choose the TX power equal to 1mW to ensure

TABLE II
10% OUTAGE SNR, IN DB, FOR 1MW TX POWER

| RX → | F | B | L | R |
|---|---|---|---|---|
| TX Front | 5.84 | 7.47 | 5.88 | 10.01 |
| TX Back | 8.91 | 9.13 | 7.92 | 9.09 |
| TX Left | 6.84 | 7.64 | 7.36 | 8.67 |
| TX Right | 7.85 | 5.24 | 7.15 | 7.66 |

that this critical SNR level is obtained for every SISO link during 90% of the time as presented in Table II.

The SISO- and MIMO-OFDM capacities vary over time and this time varying behaviour is visualized by means of a Cumulative Distribution Function (CDF), shown in Fig. 4.

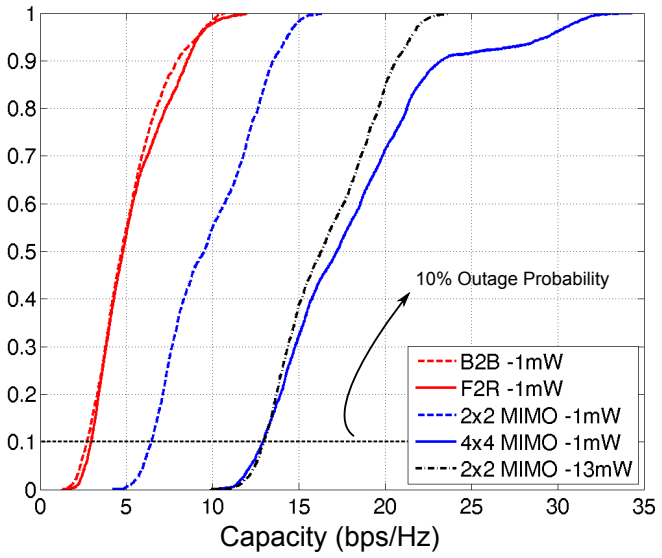


Fig. 4. Cumulative Distribution Function of the capacity, in bps/Hz

Consider the 10% outage capacity $\bar{C}_{\text{OFDM,out,10}}$, being the capacity guaranteed during 90% of the time, as indicated in Fig. 4. These 10% outage capacities provide an indication of the multiplexing and array gain obtained by both MIMO techniques, visible by a shift to the right of the CDFs. We first determine the strongest SISO links to calculate the minimal multiplexing gain when applying MIMO. These strongest SISO channels, serving as a reference point, are the B2F or F2R link for $2 \times 2$ MIMO or $4 \times 4$ MIMO respectively, where we only use the front and back antennas when applying $2 \times 2$ MIMO. Table III presents the 10% outage capacity for all sixteen SISO

links as well as for $2 \times 2$ MIMO and $4 \times 4$ MIMO.

TABLE III
10% OUTAGE CAPACITY $\bar{C}_{\text{OFDM,OUT,10}}$, IN BPS/HZ, FOR 1MW TX POWER

| | SISO | | | | MIMO | |
|---|---|---|---|---|---|---|
| RX $\rightarrow$ | F | B | L | R | 2x2 | 4x4 |
| TX Front | 1.89 | 2.24 | 1.93 | **2.97** | 6.46 | 12.92 |
| TX Back | 2.64 | **2.71** | 2.37 | 2.67 | | |
| TX Left | 2.12 | 2.31 | 2.25 | 2.60 | | |
| TX Right | 2.36 | 1.76 | 2.20 | 2.34 | | |

Table III shows that both $2 \times 2$ MIMO and $4 \times 4$ MIMO outperform each of their corresponding SISO links. This leads to a multiplexing gain equal to 3.75 bps/Hz or 9.95 bps/Hz when applying $2 \times 2$ MIMO or $4 \times 4$ MIMO respectively. Moreover, when comparing $4 \times 4$ MIMO to $2 \times 2$ MIMO, we notice a large addtional multiplexing gain equal to 6.46 bps/Hz, demonstrating the extra benefits when applying $4 \times 4$ over simple $2 \times 2$ MIMO. Furthermore, as indicated on Fig. 4, we need 13mW transmit power to achieve approximately the same 10% outage capacity for $2 \times 2$ MIMO compared with the 10% outage capacity achieved for $4 \times 4$ MIMO when only using 1mW TX power. This shows that, when applying $4 \times 4$ MIMO, the transmit power could be drastically decreased, maintaining the same throughput. Moreover, when using the on-body locations for the four transmit and receive antennas as in this paper, there is always one TX-RX antenna pair which is pointing towards each other, considering the 3dB beamwidth of the radiation pattern being $46^\circ$ in the XZ-plane and $117^\circ$ in the YZ-plane as in Fig. 1, regardless of both firefighter orientations. This increases the link reliability and avoids that body shadowing heavily decreases link quality. Note that the calculated capacities are largely independent of frequency [16], so the results can be extended to both the lower 2.45 GHz Industrial, Scientific and Medical (ISM) band [17] and the higher 5 GHz Wi-Fi band [18].

## VI. CONCLUSION

In this paper, real-life firefighter rescue operations were replicated, from which the SISO- and MIMO-OFDM capacities are calculated for realistic indoor broadband body-to-body communication channels. By means of the RMS delay spread and 50% correlation bandwidth, derived from sixteen individual SISO links, the IEEE 802.11 ac standard is proven very suitable for indoor broadband body-to-body communication. Moreover, when the TX power is only 1mW, guaranteeing realiable timing synchronisation and frequency offset estimation, channel capacities equal to 6.92 bps/Hz or 12.94 bps/Hz are obtained for $2 \times 2$ MIMO or $4 \times 4$ MIMO respectively, during 90% of the time, without the necessity of channel feedback. This corresponds to a data rate equal to 138 Mbps for $2 \times 2$ MIMO or even 259 Mbps for $4 \times 4$ MIMO when using 20 MHz OFDM bandwidth, corresponding to the smallest OFDM bandwidth defined in the 802.11 ac standard. These data rates are largly sufficient, even with a code rate of 1/2, to ensure efficient communication of crucial information between firefighters. Moreover, by improving from $2 \times 2$ MIMO to $4 \times 4$ MIMO transmit power can be drastically decreased by a factor 13.

## ACKNOWLEDGMENT

The authors would like to acknowledge IAP BESTCOM and UCL for providing the Elektrobit channel sounder and measurement locations.

## REFERENCES

[1] "Firefighter fatalities in the United States - 2013," National Fire Protection Association - Fire Analysis and Research Division, Tech. Rep., June, 2014.

[2] "802.11ac," IEEE Standard for Information technology - Telecommunications and information exchange between systems - Local and metropolitan area networks - Specific requirements - Part 11: Wireless LAN Medium Access Control (MAC) and Physical Layer (PHY) Specifications - Amendment 4: Enhancements for Very High Throughput for Operation in Bands below 6 GHz, Tech. Rep., 2013.

[3] S. Cotton and W. Scanlon, "Channel characterization for single- and multiple-antenna wearable systems used for indoor body-to-body communications," *IEEE Transactions on Antennas and Propagation*, vol. 57, no. 4, pp. 980–990, April 2009.

[4] R. Rosini, R. Verdone, and R. D'Errico, "Body-to-Body Indoor Channel Modeling at 2.45 GHz," *IEEE Transactions on Antennas and Propagation*, vol. 62, no. 11, pp. 5807–5819, November 2014.

[5] Y. Wang, I. Bonev, J. Nielsen, I. Kovacs, and G. Pedersen, "Characterization of the indoor multiantenna body-to-body radio channel," *IEEE Transactions on Antennas and Propagation*, vol. 57, no. 4, pp. 972–979, April 2009.

[6] M. Sudjai, L. C. Tran, and F. Safaei, "Performance analysis of STFC MB-OFDM UWB in WBAN channels," in *Proceedings of the 23rd IEEE Workshop on Personal Indoor and Mobile Radio Communications (PIMRC)*. Sydney, Australia: IEEE, September 2012, pp. 1710–1715.

[7] Q. H. Abbasi, A. Sani, A. Alomainy, and Y. Hao, "On-body radio channel characterization and system-level modeling for multiband OFDM ultra-wideband body-centric wireless network," *IEEE Transactions on Microwave Theory Techniques*, vol. 58, no. 12, pp. 3485–3492, December 2010.

[8] S. Lemey and H. Rogier, "SIW textile antennas as a novel technology for UWB RFID tags," in *Proceedings of RFID Technology and Applications Conference (RFID-TA)*. Tampere, Finland: IEEE, September 2014, pp. 256–260.

[9] R. Janaswamy, *Radiowave Propagation and Smart Antennas for Wireless Communications (The Springer International Series in Engineering and Computer Science)*. Springer, 2000.

[10] G. Janssen, P. Stigter, and R. Prasad, "Wideband indoor channel measurements and BER analysis of frequency selective multipath channels at 2.4, 4.75, and 11.5 GHz," *IEEE Transactions on Communications*, vol. 44, no. 10, pp. 1272–1288, October 1996.

[11] A. Goldsmith, *Wireless Communications*. Cambridge University Press, 2005.

[12] Y.-Q. Jiang, "Accurate capacity analysis for MIMO-OFDM systems considering correlation between subcarriers," in *Proceedings of the IEEE 12th International Conference on Communication Technology*. IEEE, November 2010.

[13] Y.-C. Liang, R. Zhang, and J. Cioffi, "Transmit optimization for MIMO-OFDM with delay-constrained and no-delay-constrained traffic," *IEEE Transactions on Signal Processing*, vol. 54, no. 8, pp. 3190–3199, August 2006.

[14] H. Suzuki, T. V. A. Tran, and I. B. Collings, "Characteristics of MIMO-OFDM channels in indoor environments," *EURASIP Journal on Wireless Communications and Networking*, vol. 2007, no. 1, pp. 1–9, December 2006.

[15] E. Zhou, X. Zhang, H. Zhao, and W. Wang, "Synchronization algorithms for MIMO OFDM systems," in *IEEE Wireless Communications and Networking Conference*, vol. 1, March 2005, pp. 18–22 Vol.

[16] P. Rysavy, "Challenges and considerations in defining spectrum efficiency," *Proceedings of the IEEE*, vol. 102, no. 3, pp. 386–392, March 2014.

[17] "Electromagnetic compatibility and Radio spectrum Matters (ERM); Wideband transmission systems; Data transmission equipment operating in the 2,4 GHz ISM band and using wide band modulation techniques," European Telecommunications Standards Institute, Tech. Rep., April 2004.

[18] "FCC Increases 5GHz Spectrum for Wi-Fi, Other Unlicensed Uses," Federal Communications Commission, Tech. Rep., 2014.